

EBHIS Technical Report

Benjamin Winkel Lars Flöer Jürgen Kerp

January 10, 2011

We report on the data quality and various observational difficulties encountered while using the 21-cm seven-feed receiver at the 100-m telescope for the Effelsberg-Bonn HI Survey (EBHIS) observations since late 2008.

1 Overview

In this report we summarize the current status of the EBHIS in terms of data quality and technical issues encountered during the measurements in the last two years. Currently, the three main issues with the EBHIS are radio frequency interference (RFI; Section 2), bandpass calibration, and standing-waves. The latter two are closely related problems in terms of data reduction though being physically independent. They are described in Section 3. In Sections 4 and 5 our observing strategy is discussed taking into account the technical framework defined by the instrument. Finally, in Section 6 a brief overview of the current EBHIS status and data quality will be given, followed by a short summary (Section 7).

2 Radio Frequency Interference (RFI)

2.1 Regular Interference

EBHIS data shows numerous narrowband and a considerable number of broadband interference signals. Whereas the latter mainly occur in the frequency range that is allocated to aeronautical radio navigation, the former are present all over the observing band and even in the protected part of the L-band; see Fig. 1.

Narrowband interference pollutes mostly one or two adjacent spectral channels and has in many cases rather constant amplitudes over a few minutes. Furthermore, interference in a given spectral channel and therefore frequency is visible in all 14 basebands of the 7-beam receiver. In many cases the amplitude of a given interference signal is different across the basebands. Often, narrowband RFI spikes appear in a comb-like pattern with equidistant frequencies (also in Fig. 1) which makes it likely that these spikes share

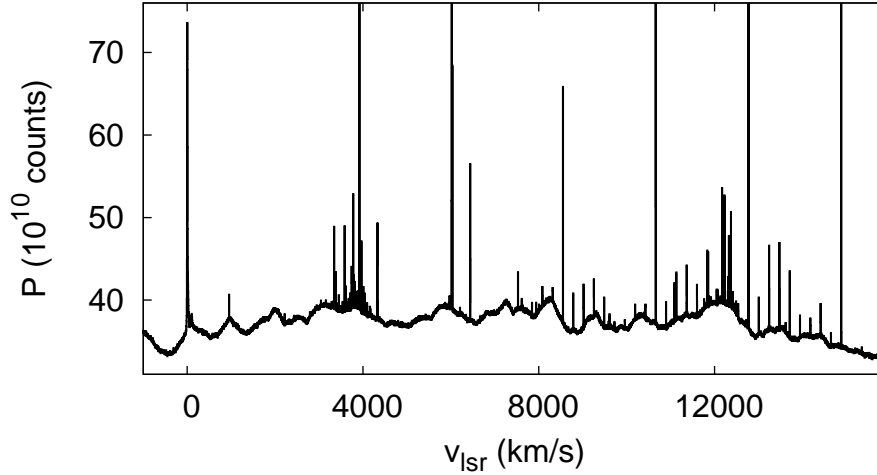


Figure 1: Typical raw spectrum of the EBHIS observations. Except for the emission line at $v_{\text{lsr}} \approx 0 \text{ km s}^{-1}$ all other narrow features can be attributed to RFI. The underlying baseline has a highly complex shape making correction difficult.

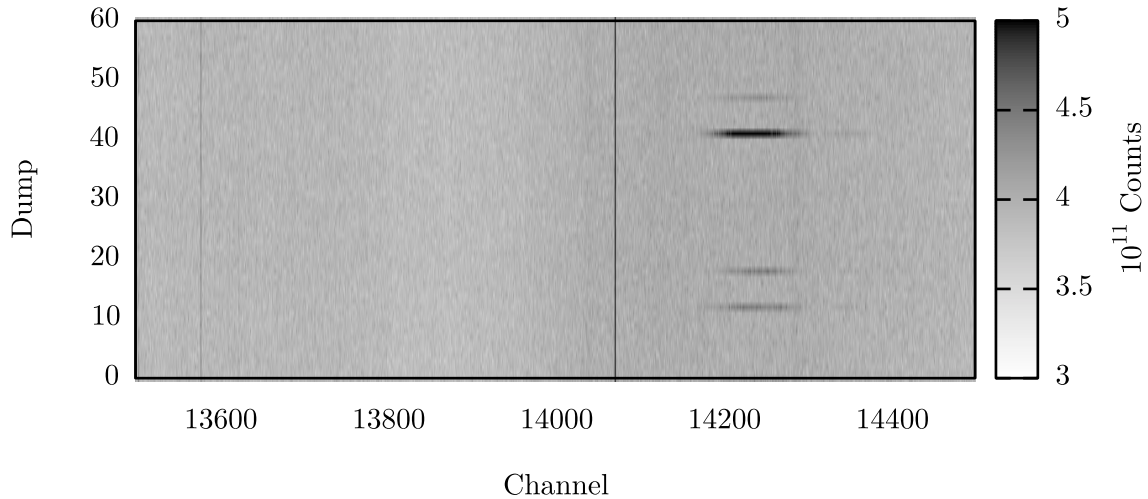


Figure 2: Signature of broadband interference in raw data.

a common origin. Two bands in the spectra (at about 1403 MHz and 1363 MHz, or $v_{\text{lsr}} \approx 4000 \text{ km s}^{-1}$ and 12500 km s^{-1} , respectively) each being approximately 500 spectral channels wide are polluted with lots of individual RFI spikes. Except for these two bands narrowband RFI covers only a small fraction of all data (in the time–frequency plane) such that even in the case of complete excision of bad data points one loses only about 5% of the data. Broadband interference is relatively unproblematic for observations since it occupies very little data and can be efficiently mitigated. The signature of the two types of interference is illustrated in Fig. 2 and 3.

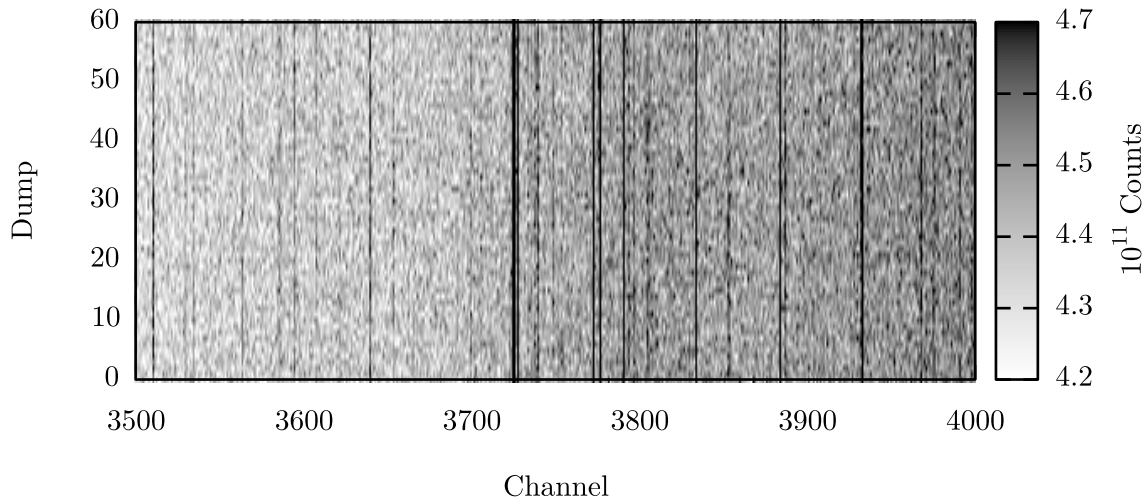


Figure 3: Signature of narrowband interference in raw data.

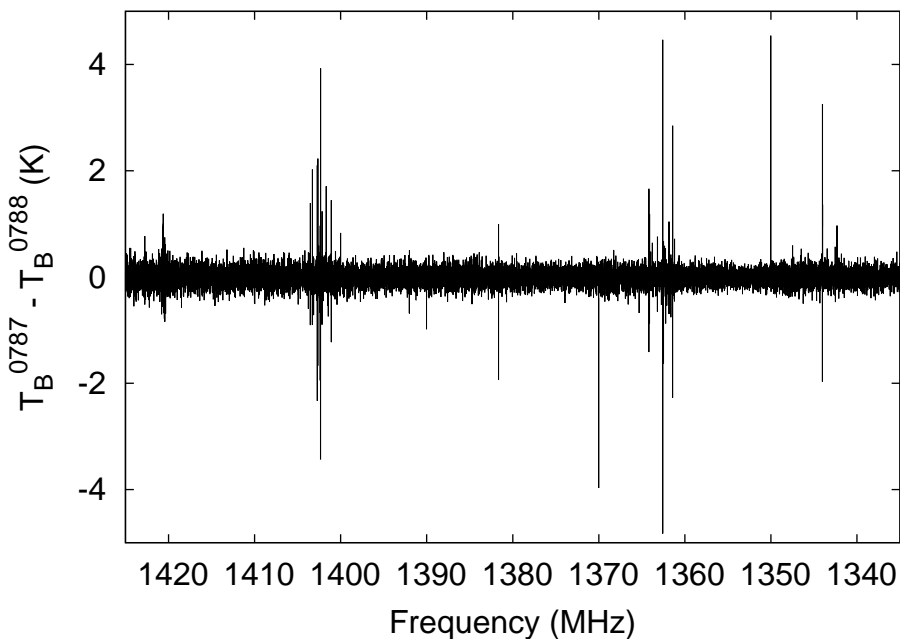


Figure 4: The amplitudes of narrowband RFI appear to be rather constant on short timescales. The plot shows the difference spectrum of two measurements of the calibration source S7 performed within 3 min time delay. Only few (strongly time-variable) emitters appear mainly located within two bands at about 1403 MHz and 1363 MHz. Note, that both spectra ($\tau = 2$ min) were independently calibrated (for gain and bandpass) and baseline-corrected before the difference spectrum was calculated.

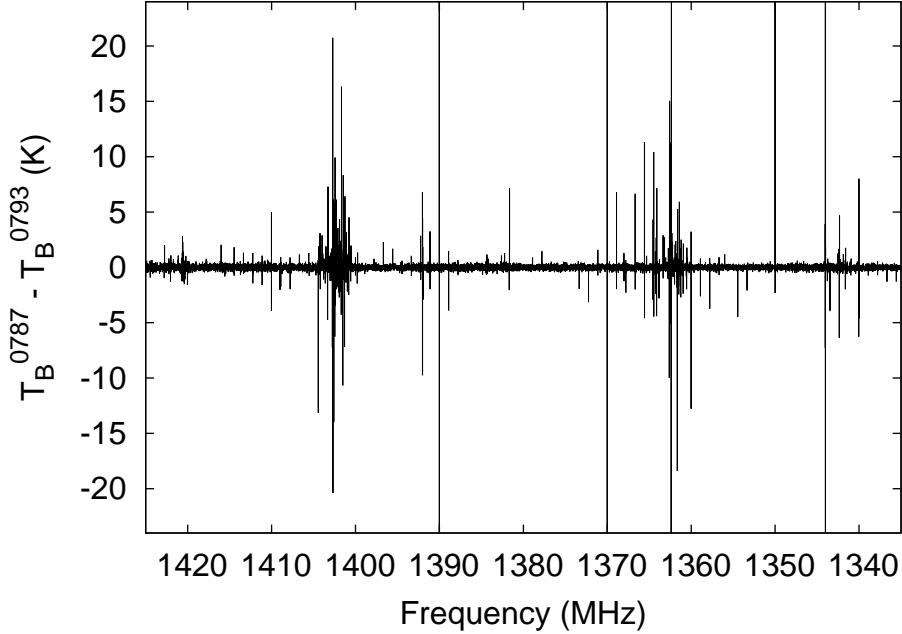


Figure 5: In contrast to Fig. 4, the RFI situation changes drastically on the course of several hours. Again two S7 measurements were utilized but this time with a gap of 5 h between the observations.

While most narrowband RFI signals of a given baseband appear rather constant in amplitude within short time intervals (during a subscan, i.e., few minutes) as is shown in Fig. 4 the RFI situation changes significantly during an observing session of several hours length; see Fig. 5. Hence, the amount or amplitudes of the interference signals is likely dependent on azimuth, elevation, and/or time. Furthermore, most RFI is strongly polarized (Fig. 6).

During test measurements in spring 2009 with the help of telescope staff members we searched for RFI sources at the site. These measurements suggested, that the amplitude of many narrowband RFI signals would increase when the doors of the secondary focus were left open, which eventually would hint to RFI emitters being located in the secondary focus. We repeated similar tests during January 2011, but could not confirm this finding. Nevertheless, in contrast to the usual finding of RFI amplitudes being constant on short time intervals the opened doors do change the interference levels, but not generally in a manner where open doors mean higher levels; see Fig. 7. While the new test was performed at relatively low elevation the previous measurement was performed in Zenith. In the latter case the open doors might have reflected RFI from the horizon into the feed horns more efficiently, mimicking RFI sources in the secondary focus.

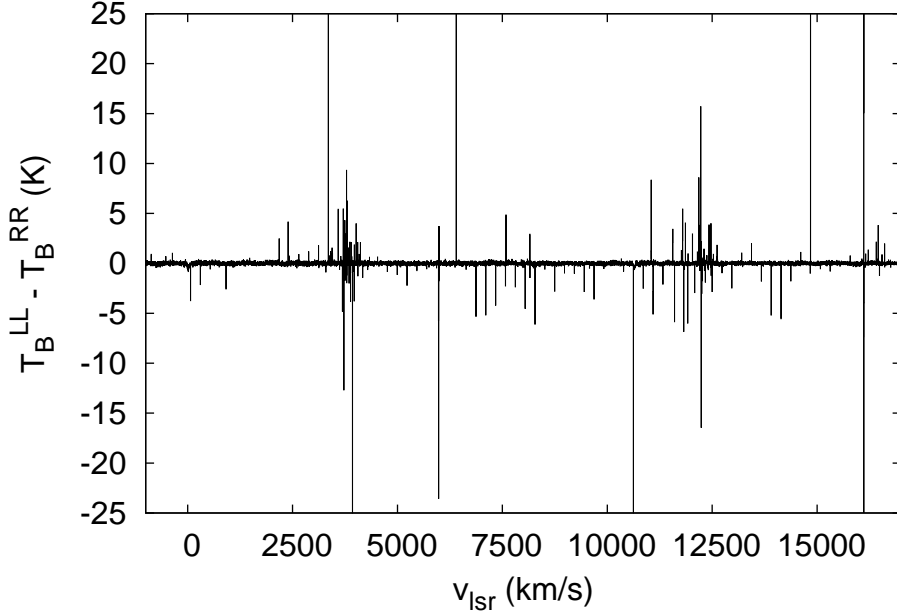


Figure 6: Most RFI signals are strongly polarized. The plot displays the difference between left- and right-hand circular polarization of the central feed for one measurement.

2.2 Persistent Broadband RFI

Since spring 2009, EBHIS observations were subject to persistent broadband interference in the azimuthal range between 220° and 340° . This RFI signal manifests itself in strong variations of the baselines in three different bands of about 10 MHz each; see Fig. 8. The three regions affected are:

- above 1420.2 MHz
- 1396.4 to 1405.6 MHz
- 1350.7 to 1362.9 MHz.

This in turn leads to a wave-like pattern in the position–velocity representation of the EBHIS data cubes (see Fig. 9). This modulation of the baselines is so severe that the data contaminated with this type of interference is not usable for science and has to be discarded. The dependence on the azimuth is illustrated in Fig. 10. As a consequence we had to limit all observations to an azimuthal range far off the affected region.

The azimuth range clearly favors the direction of the main building, especially the southern part of it. We therefore suspect that this certain type of interference stems from an electronic device in the main building. The spectral shape of the interference makes it hard to limit the possible sources, but the broad band characteristic clearly favors an analog device, since digital signals are more confined in frequency.

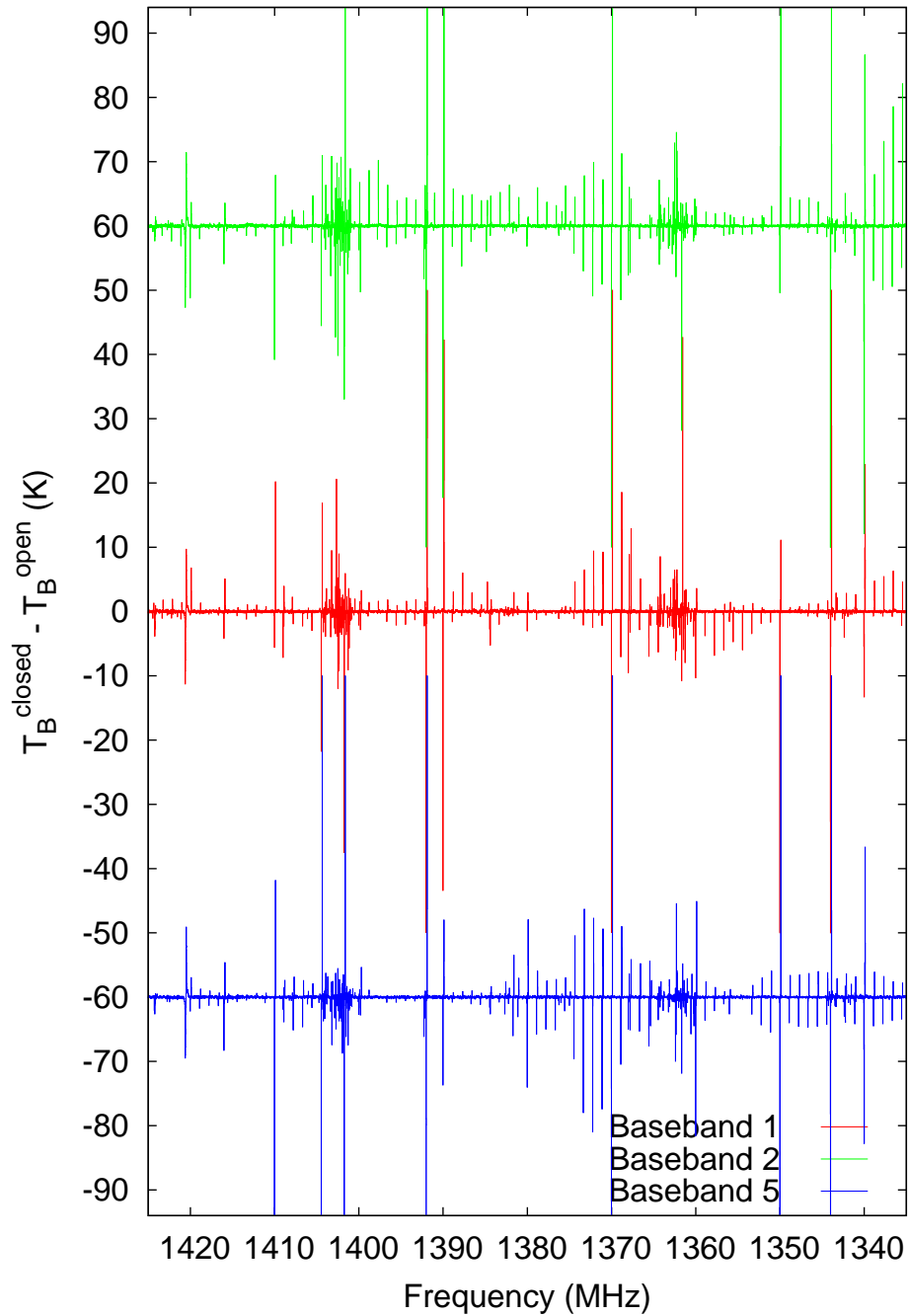


Figure 7: Difference of narrowband RFI amplitude levels with closed and open doors of the secondary focus cabin. Although the two measurements were performed with only 10 min time difference the changes are rather large. This is most likely due to the changed aperture causing different reflection paths for RFI. Three different basebands are shown.

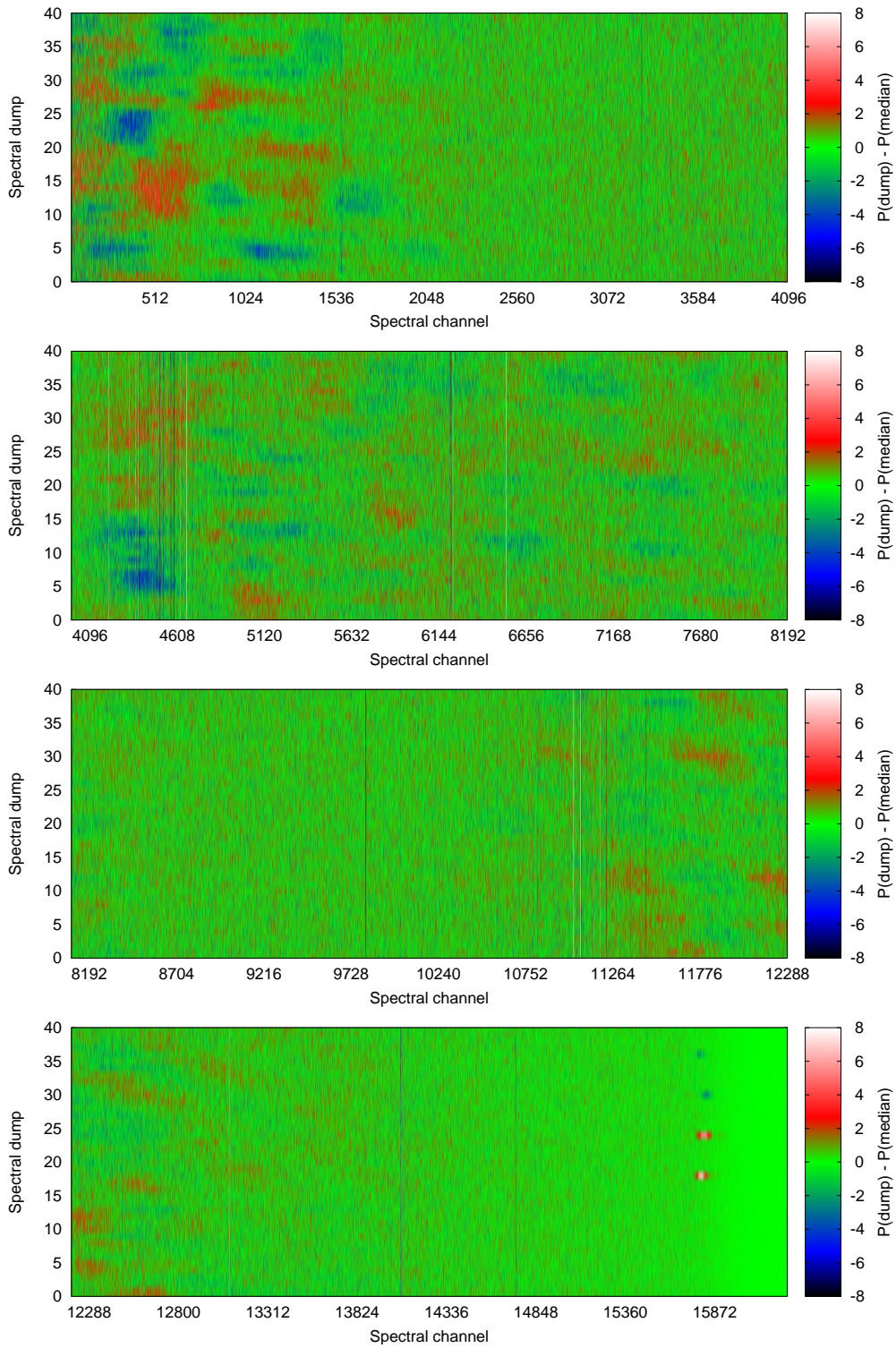


Figure 8: Signature of the persistent broadband interference in the raw data. Three regions are affected: (1) above 1420.2 MHz (spectral channel 0 to 1600); (2) 1396.4 to 1405.6 MHz (spectral channel 4000 to 5500); (3) 1350.7 to 1362.9 MHz (spectral channel 11000 to 13000).

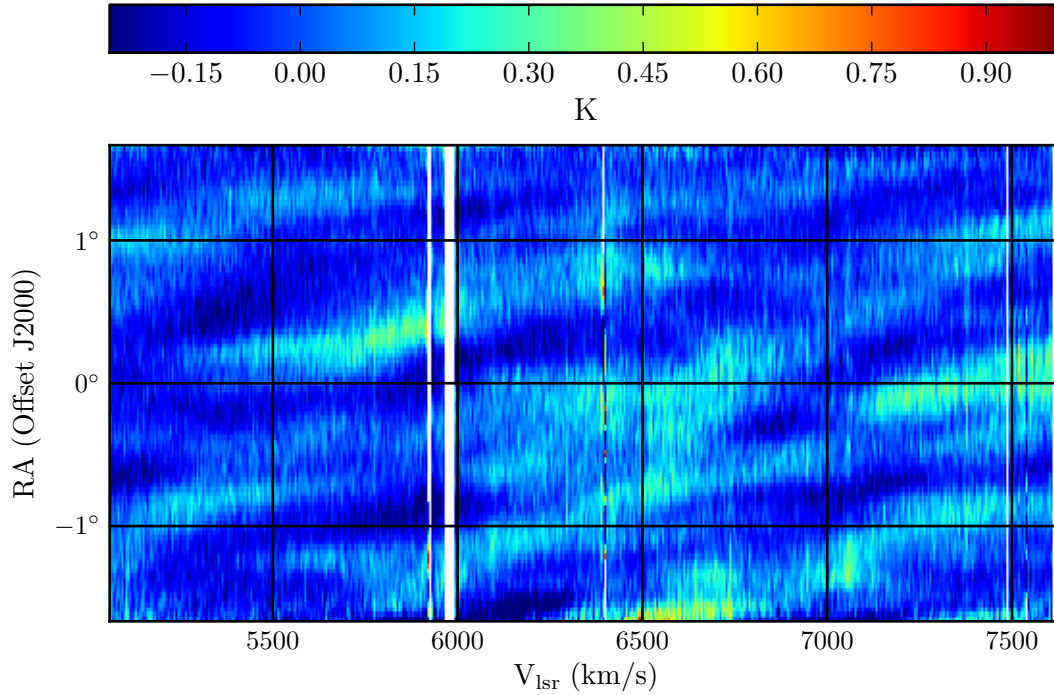


Figure 9: In the final data cubes the persistent broadband interference leads to a wave-like pattern in the position–velocity representation.

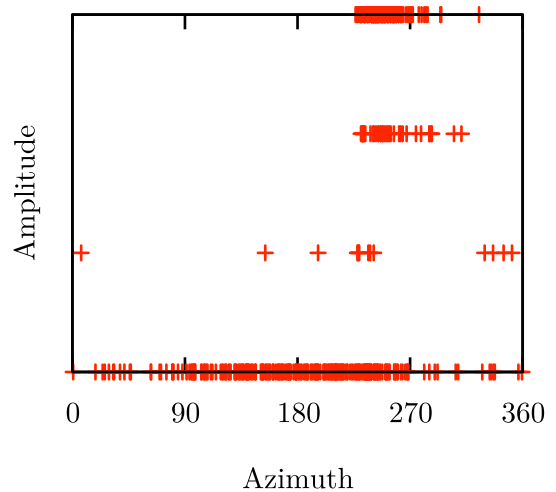


Figure 10: Classification of current EBHIS measurements according to the severity of the persistent broadband interference as a function of azimuth.

2.3 Low-level Narrowband Interference

During deep ($\tau = 600$ s/beam) observations in the direction of the Virgo Cluster, it became evident, that there is a high abundance of low-amplitude narrowband interference; see Fig. 11 top panel. This interference is not visible in the usual EBHIS observations ($\tau = 36$ s/beam).

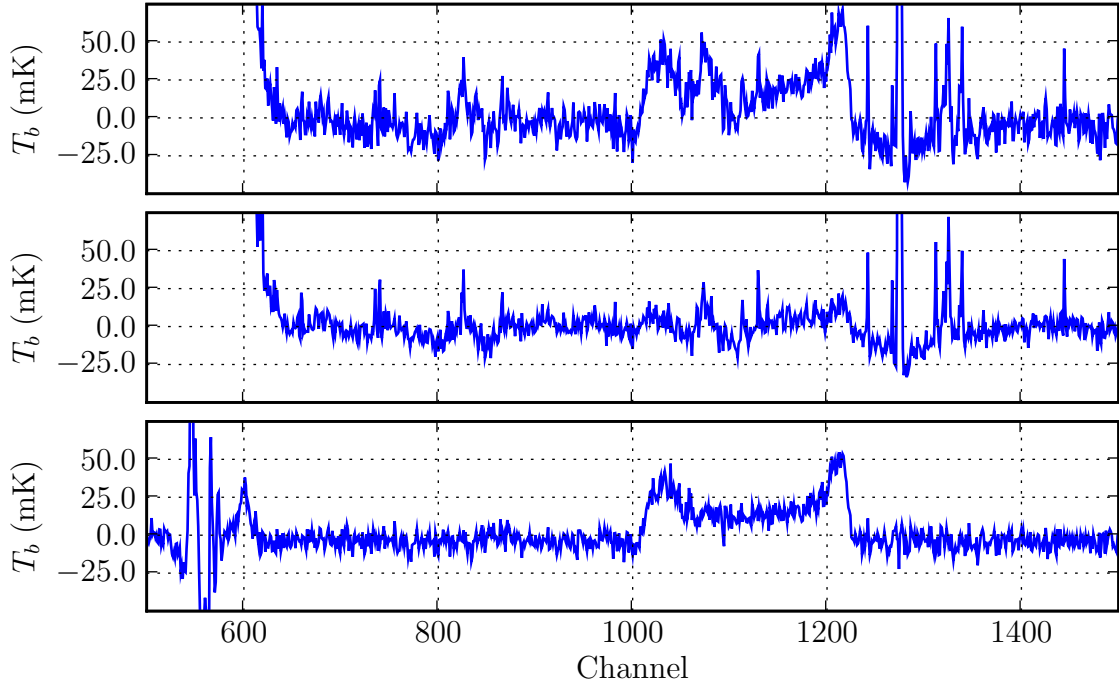


Figure 11: Spatially averaged spectrum of a galaxy from the deep observations of the Virgo Cluster. The top panel shows the data quality from the data reduction pipeline. The middle panel shows the result from the median filter. The bottom panel is the difference between the top and middle panel. Note that the filter also affects the source shape.

Due to the high abundance of the low-level interference, the reduced data has an RMS of 15.4 mK, almost three times higher than the value obtained from the radiometer equation of 5.4 mK ($T_{\text{sys}} = 40 \text{ K}$ ¹, $\Delta v = 10 \text{ km/s}$). Only when applying a filter that suppresses the low-level interference, the RMS can be reduced to 6.2 mK, which is close to the theoretical value. This filter uses a median estimator to filter out the spatially extended signature of the narrowband interference in the final data cubes; see Fig. 11 middle panel. However, it also affects the source signal in the data (Fig. 11 bottom panel), and should therefore only be seen as a quick fix rather than a permanent solution.

Since low-level interference has the same spectral signature as the more intense narrowband interference a common source seems likely. Whereas in normal EBHIS observations the RFI environment in the L-band at Effelsberg is sufficiently well-behaved, it is difficult to obtain high quality deep observations due to the high abundance of interference.

¹The observations of the Virgo Cluster were carried out at rather low elevations, due to the constraints placed on the azimuth due to the interference described in Section 2.2.

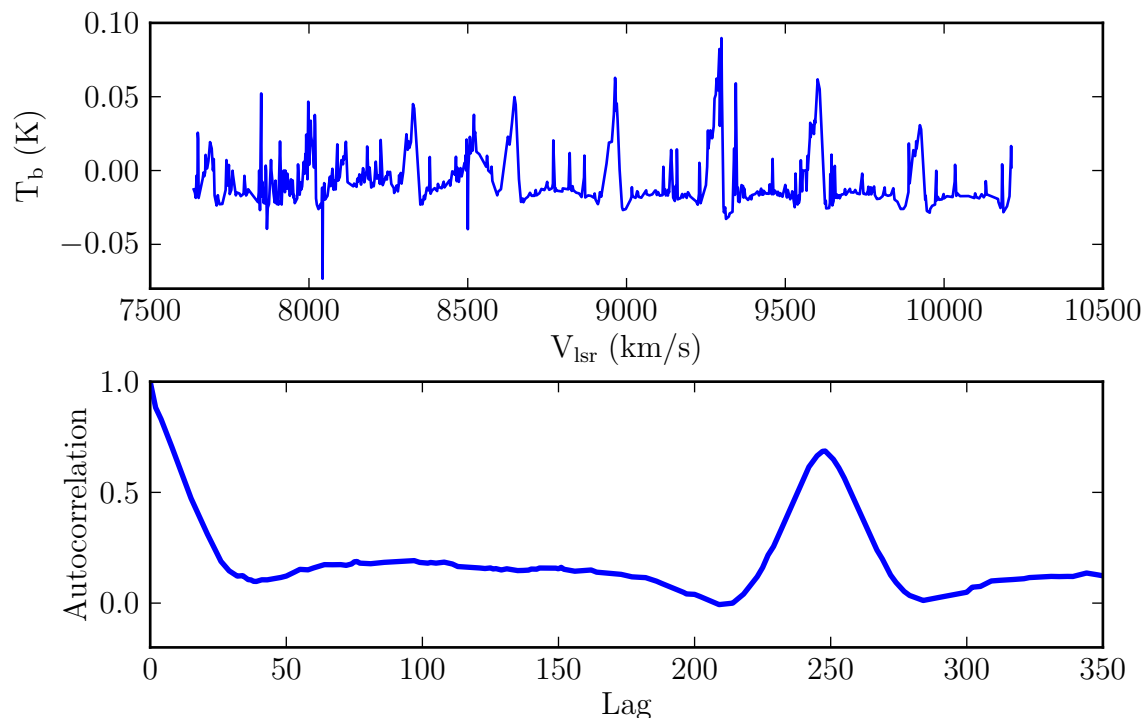


Figure 12: Top panel: Average spectrum over the high redshift part of a whole dataset. Remaining low-level RFI and the periodic interference signal are clearly visible. Bottom panel: Autocorrelation of the data in the top panel. The peak of the autocorrelation at 247 corresponds to a period of about 1.5 MHz.

2.4 Other Interference

2.4.1 GPS L3 Mode

A recent addition to the Global Positioning System, GPS, added a new carrier frequency at 1381.05 MHz. This signal is especially problematic because it has a large bandwidth of 1 MHz or roughly 220 km/s and overlaps with the HI emission at the redshift of the Coma cluster [2]. Since this GPS signal is part of a military nuclear event detection system, it is not announced beforehand and measurements corrupted with this signal have to be discarded. Flagging of this interference is especially difficult because it exhibits very large side lobes that affect a large portion of the observing band. The current approach is to just discard a large amount of the affected data.

2.4.2 1.5 MHz Periodic Interference

During the previously mentioned observations of the Virgo Cluster, a spectrally broad interference signal ($\Delta v \approx 20$ km/s) was detected. This signal repeated quite precisely every 1.5 MHz, as confirmed by the autocorrelation function of the spectra (see Fig. 12).

3 Baseline issues

A very important aspect of the EBHIS survey is the ability to reduce a large amount of spectra in an automatic fashion which made it necessary to develop new fast and robust algorithms. Apart from RFI excision the second major computationally expensive task is the baseline calibration. During our measurements it turned out, that the complex shape of the underlying baseline in the spectra (compare Fig. 1) is the result of two very different effects. The first is the bandpass (or gain curve), the second is strong multi-modal standing waves produced in the primary-secondary dish ‘resonator’ of the telescope.

The bandpass of the system is a frequency-dependent gain that, hence, acts in a multiplicative way on the signal fed into the receiver. As such it is important not to confuse the overall baseline with the bandpass, as additive signals like the standing waves show also a strong frequency dependence but are further multiplied with the frequency-dependent bandpass. As a consequence, effort has to be taken to separate both functions and treat them individually.

3.1 Bandpass ripples

In order to extract the true bandpass shape one usually applies techniques like position of frequency switching. However, as we show in [4] both methods will fail in the presence of a strong frequency dependence of the RF part of the bandpass (i.e., before the down conversion in the mixer). Unfortunately, it turned out that the seven-feed receiver has a very strong RF frequency dependence.

To calculate the true bandpass shape $G = G_{\text{RF}}G_{\text{IF}}$ (of the combined RF/IF system) we utilize a new method using the built-in noise diode. According to Keller (*priv. comm.*) the frequency curve of which is sufficiently flat, such that we can compute

$$\begin{aligned} P_{\text{IF}}^{\text{cal}} - P_{\text{IF}} &= G [T_{\text{A}}^{\text{cal}} + T_{\text{sys}}^{\text{cal}} + T^{\text{cal}} - T_{\text{A}} - T_{\text{sys}}] \\ &= GT^{\text{cal}} \end{aligned} \tag{1}$$

which allows to compute G as a function of the raw spectra deterministically. As we dump spectra on very short time scales the resulting G is too noisy to be used. A well-working solution is to calculate the mean spectra (or median spectra to avoid influence of bursts of RFI) over several hundreds or even a few thousands of seconds, e.g., using a complete 5×5 sq.deg. map (for each baseband).

In Fig. 13 we show an example bandpass curve containing several ripples which do follow the LO shift strongly suggesting the origin of these ripples to be located in the RF part of the receiver. Furthermore, a zoom-in (Fig. 14) reveals rather sharp features the reason of which is currently unknown.

The bandpass curves are similar (not identical) in all basebands except for two: baseband 7 and 14; see Fig. 15 for an example. These two basebands (from the same feed) show a strong feature in the center of the bandpass. The functional form of the bandpass curves is rather stable with time, although some of the features (especially the more sharp ones) vary slightly over the course of few hours to days.

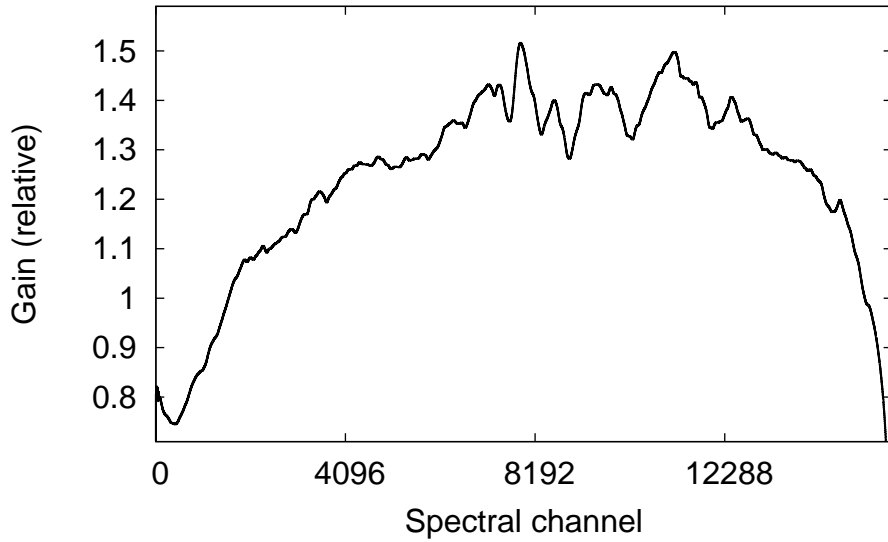


Figure 13: Bandpass curve $G = G_{\text{RF}}G_{\text{IF}}$ of the complete 21-cm multi-feed system (base-band 1). The ripples (see Fig. 14 for a zoom-in) are caused by the RF part of the heterodyne receiver, as they follow the LO shift.

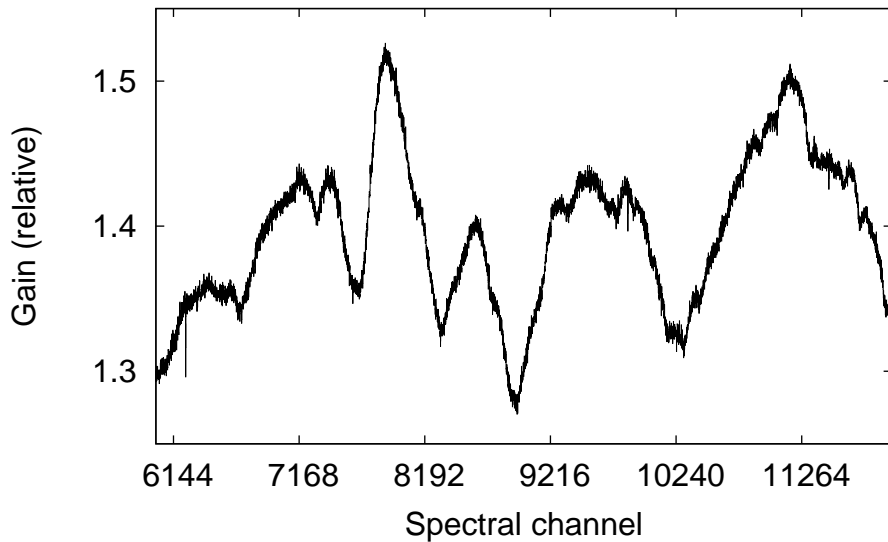


Figure 14: Zoom-in of the bandpass curve in Fig. 13.

As a final remark we like to point out, that also the single-feed 21-cm receiver (which is very similar to the multi-feed system) shows the strong RF ripples, as could be confirmed by test measurements.

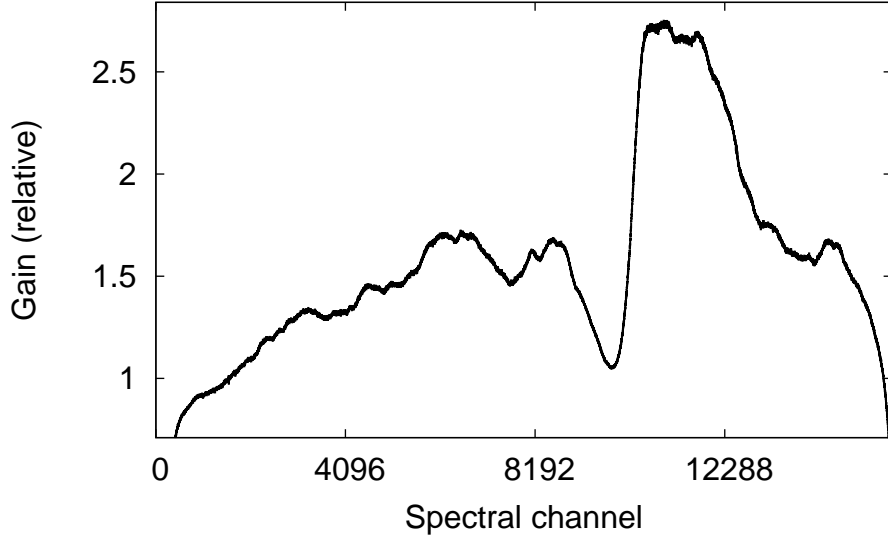


Figure 15: As Fig. 13 but showing the bandpass of baseband 14 which contains a strong jump, the origin of which is unknown.

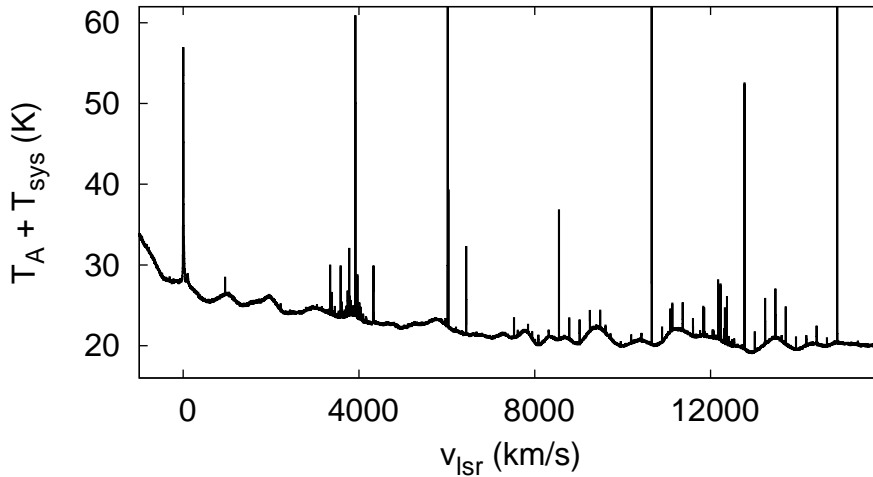


Figure 16: Reconstructed spectrum after bandpass and gain calibration. The remaining baseline level is due to the various continuum and noise contributions modulated with a multi-modal sine-wave pattern (standing waves).

3.2 Standing waves

After application of the bandpass removal (i.e., division of the spectra with the determined bandpass curve) the spectra also reveal multi-modal sine-wave contributions; see Fig. 16. Usually, such a pattern is attributed to standing waves (SWs) between the primary and secondary focus. We tested this hypothesis by performing test measurements with the single-feed receiver (which is constructed in a similar way as the multi-feed).

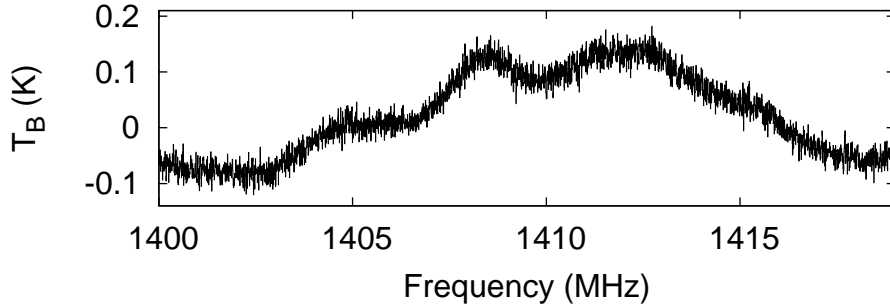


Figure 17: In the final data cubes residual imprints of the standing waves are still visible in some cases, e.g., on bright continuum sources. The plot shows the spectrum of M 86 in a data cube corrected for baseline and continuum. Apart from such defects the data cubes have sufficiently flat baselines.

For technical reasons the sub-reflector at the 100-m telescope is slightly off-axis when observing with this instrument. These tests showed a significant reduction of the SW amplitudes.

The different baselines show generally different standing wave patterns which slowly change during the measurements most likely as a result of a changing continuum level. This can be clearly seen in the final data cubes where strong continuum sources exhibit a residual wave-like pattern; see Fig. 17. As the baselines are computed for complete subscans to increase accuracy, the algorithm can not account for rapid changes in the baseline. But even slightly different continuum levels (e.g., due to changing ground radiation) will have some (statistical) impact. This imposes a serious problem to the baseline computation because the commonly utilized approach — computing median baselines for a certain time interval — will not be able to remove residual changes in the SW. In some cases data cubes produced using median baselines show clear signs of a SW pattern. Currently the only solution for the EBHIS is the application of computationally expensive two-dimensional FFT filtering algorithms directly applied to the time–frequency plane. A drawback are so-called baseline holes which can be produced around weak astronomical sources which could not be flagged automatically. **Therefore, a solution to the SW problem would be of special importance for the EBHIS both in terms of data quality and processing time.**

4 Instrumental setup and map planning

In order to minimize the effects imposed by RFI, bandpass, and standing waves issues the following measurement scheme emerged. Survey observations are carried out in smaller portions mapping 5×5 sq.deg. fields per Scan (each map takes about 65 to 70 min of observing time). The individual maps are measured in so-called zig-zag on-the-fly mode (scanning in Right ascension). In principle mapping at constant elevations would probably result in much less SW residual changes but it would be much more difficult

to obtain a homogeneous noise level (i.e., integration time per position) across the sky.

Due to the extremely broadband RFI (see Section 2.2) we limit all observations (except of the calibration source S 7) to the azimuthal range between 30° and 200° . The limitation in azimuth has the disadvantage, that observations have to be carried out before the culmination of a given field which leads to a higher system temperature because of the low elevation, especially for the fields at low declination. Also, the possibility to obtain a second coverage of the target fields at a different hour angle and therefore velocity correction is highly limited. Such a coverage is highly advantageous when it comes to the elimination of systematic errors and RFI mitigation.

A second limitation is caused by the mapping speed. In order to achieve the desired 36s of integration time per beam the individual maps utilize a scanning speed of $240''$ per second. At elevations above 60° this starts to exceed the specified maximal telescope speed². Hence, all observations have to be allocated to obey both limits, making map planning a relatively complex task. A special simulation software was written to assist the observer with finding appropriate LST intervals for certain sky fields.

Initially, we intended to use the common frequency-switching technique to obtain bandpass-calibrated spectra. As discussed above, this is not feasible with the current front-end. For consistency of all data taken so far we decided to still use the four-phase switching scheme (i.e., using cal/nocal and two different LO shifts), although we do not utilize the switched spectra for bandpass correction.

One important point is, that for our bandpass calibration method, the noise diode with the higher noise temperature must be used. Several tests have been carried out with the lower noise temperature diode and we were not able to calculate the bandpass shapes to sufficient accuracy.

5 Telescope control software

During Summer 2010 a new telescope control software was implemented at Effelsberg. In the meantime most of the initial issues related with the new software could be resolved. Currently, there is one issue with the “Fitswriter” task which connects with the backend server to receive the raw spectral data and write them to disk. A special version of the control software was forked to circumvent this issue (`affts_control.py`).

A problem which only occurred in the beginning of the EBHIS campaign (with the old control software, which was later also fixed) was that the feed rotation angle (aka OPOS) which should account for the parallactic angle changes during the measurement was wrongly calculated. As a consequence some of the measurements suffer from strong aliasing rendering the data virtually unusable.

²Also the differential change of the parallactic angle must not exceed certain values.

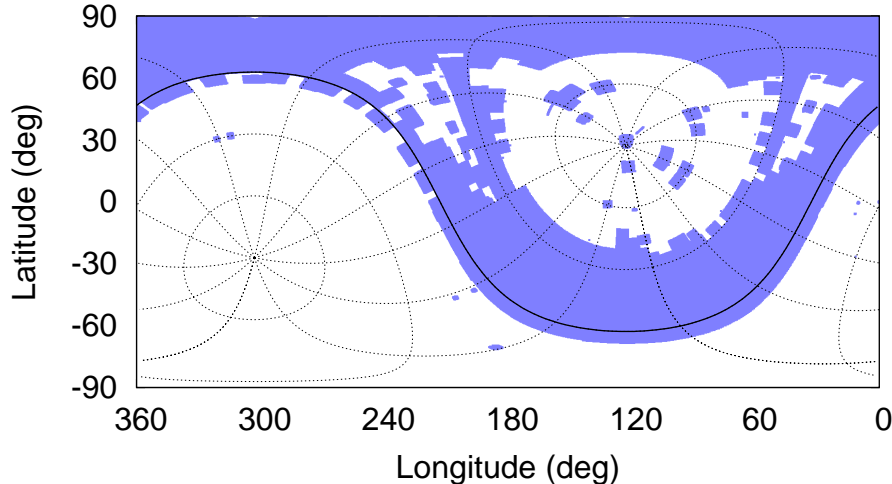


Figure 18: Current sky coverage of the EBHIS as of Nov. 2010.

6 Current status of the EBHIS and data quality

Since the beginning of 2009 the regular EBHIS measurements (i.e., the survey mode) is ongoing. For a detailed technical report of the precursor test observations see [3]. As shown earlier, the multi-feed receiver provides good system temperature values and stability. [1] performed an analysis of two deep fields (each having 10 min effective integration time per position) showing that the receiver can in principle be used for such measurements, although some special treatment of the data is necessary due to RFI and standing waves (for further details we refer to [1]).

In Fig. 18 the current sky coverage of EBHIS is shown. Unfortunately, several of the 5×5 sq.deg. maps are strongly affected by RFI and aliasing artifacts (see below). About 40% of the first coverage of the Northern hemisphere has been mapped so far (with sufficient data quality). In total about 800 h of observing time was allocated up to now, 300 h of which have to be treated as lost due to the mentioned problems (for a more detailed list, see Appendix A).

Despite all the problems with the data the first results are very promising. In Fig. 19 we show a comparison of a field measured with the Galactic All-Sky Survey (GASS, made with the Parkes telescope) and EBHIS having similar quality and sensitivity. EBHIS has a slightly higher nominal noise level but better angular resolution leading to about the same column density detection limits (when smoothing the Effelsberg beam to the Parkes resolution).

A comprehensive review on the EBHIS is given in Kerp et al. (2010 submitted).

7 Summary

Even in its incomplete shape, the EBHIS has already proven to be an extremely valuable source of high-quality data. Unfortunately, we suffer from two effects — strong

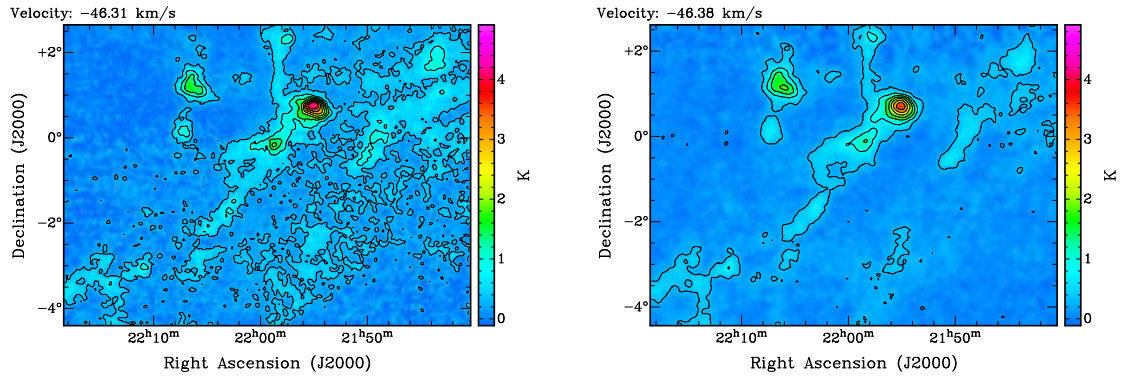


Figure 19: Comparison of a field measured with EBHIS (left panel) and GASS (right panel). Note, that the EBHIS map is actually a mosaic of four different measurements, the upper part having lower noise level (as observed with twice the integration time).

RFI pollution and a complicated standing wave pattern — making the data reduction complicated and computationally expensive. While we developed methods which are able to deal with these problems under most circumstances, especially, the search for the faintest structures in the data will not be an easy task, as low-amplitude RFI is very abundant and our baseline algorithm produces ‘holes’ adjacent to the sources. (Note, that the baseline holes are a well-known problem regardless of the specific baseline algorithm, only the relative strength of the holes could be somewhat lowered when the baselines were intrinsically more stable).

We would also like to point out, that the bandpass curve (i.e., the wiggles in the RF part) does not allow frequency switching (and would even make position switching rather complicated). This fact is probably also of interest for other observers, when using the multi-feed (and also single-feed) receiver.

Unfortunately, the source of the extremely broadband persistent RFI (see Section 2.2) was still not identified, limiting the azimuthal range which can safely be observed substantially. A solution to this issue would be very welcomed.

References

- [1] Flöer, L., 2010, Diploma thesis, *Evaluation of the EBHIS data on the local universe*
- [2] Nigra, L., Lewis, B. M., Edgar, C., Perillat, P., Quintero, L., Stanimirovic, S., & Gallagher, J. S., 2010, arXiv:1007.1801
- [3] Winkel, B., Kerp, J., & Kalberla, P. M. W., 2007, Tech. Report, *EBHIS: Test observations with the new 7-Beam receiver*
- [4] Winkel, B., Kalberla, P. M. W., Kerp, J., & Flöer, L., 2010, ApJS, 188, 488

MB0GALPOL	2009-07-18T15:13:09	1163	1	39	11h50m27s	7d19m36s	70 min	0%
C4GALPOL	2009-07-18T12:49:15	1161	1	76	13h13m44s	27d7m40s	137 min	0%
C1GALPOL	2009-07-18T11:43:56	1159	16	50	12h6m49s	27d7m40s	62 min	0%
C1GALPOL	2009-07-18T10:25:19	1148	1	16	12h6m49s	27d7m40s	28 min	0%
F0GALPOL	2009-07-18T09:11:49	1146	1	39	11h31m11s	42d2m42s	70 min	0%
B15CRIT	2009-07-18T08:05:51	1142	1	23	0h31m26s	7d40m0s	41 min	100%
B11CRIT	2009-07-18T06:53:35	1140	1	39	23h11m26s	7d40m0s	70 min	100%
B8CRIT	2009-07-18T05:40:22	1138	1	39	22h11m26s	7d40m0s	70 min	100%
B7CRIT	2009-07-18T04:26:11	1136	1	39	21h51m26s	7d40m0s	70 min	99.4%
B6CRIT	2009-07-18T03:10:38	1134	1	39	21h31m26s	7d40m0s	70 min	41.9%
B5CRIT	2009-07-18T01:56:02	1132	1	39	21h11m26s	7d40m0s	70 min	0%
B4CRIT	2009-07-18T00:37:36	1130	1	39	20h51m26s	7d40m0s	70 min	0%
F5GALPOL	2009-07-17T23:02:17	1126	1	39	13h44m46s	42d2m42s	70 min	100%
B5GALPOL	2009-07-17T20:43:11	1124	1	76	13h34m17s	22d7m40s	137 min	100%
B4GALPOL	2009-07-17T18:17:36	1122	1	76	13h12m51s	22d7m40s	137 min	69.6%
MA0GALPOL	2009-07-17T16:59:28	1120	1	39	11h50m27s	12d13m36s	70 min	19.1%
MB6GALPOL	2009-07-17T15:30:41	1117	1	39	13h52m24s	7d19m36s	70 min	0%
MB5GALPOL	2009-07-17T14:15:34	1115	1	39	13h31m57s	7d19m36s	70 min	0%
F4GALPOL	2009-07-17T12:54:18	1112	1	39	13h17m48s	42d2m42s	70 min	0%
E0GALPOL	2009-07-17T11:51:46	1110	8	39	11h41m38s	37d7m40s	58 min	0%
E0GALPOL	2009-07-17T11:09:36	1108	1	5	11h41m38s	37d7m40s	9 min	0%
A12CRIT	2009-07-17T04:00:59	1088	15	76	23h31m26s	2d45m0s	112 min	0.4%
B3CRIT	2009-07-17T02:44:49	1086	1	39	20h31m26s	7d40m0s	70 min	77.8%
B2CRIT	2009-07-17T01:28:58	1084	1	39	20h11m26s	7d40m0s	70 min	11.1%
B1CRIT	2009-07-17T00:12:08	1082	1	39	19h51m26s	7d40m0s	70 min	0%
E4GALPOL	2009-07-16T21:45:57	1080	1	76	13h16m19s	37d7m40s	137 min	100%
B2GALPOL	2009-07-16T19:26:18	1078	1	76	12h30m0s	22d7m40s	137 min	100%
AM9CRIT	2009-07-16T17:50:44	1076	1	39	16h31m27s	2d45m0s	70 min	0%
S7	2009-07-16T16:47:30	1072	1	24	8h48m0s	-1d0m0s	29 min	9%
A11CRIT	2009-07-16T04:56:14	1064	66	76	23h11m26s	2d45m0s	20 min	0%
A12CRIT	2009-07-14T04:56:27	1009	1	15	23h31m26s	2d45m0s	27 min	0%
A11CRIT	2009-07-14T04:32:20	1007	66	76	23h11m26s	2d45m0s	20 min	0%
A10CRIT	2009-07-14T02:09:08	1005	1	1	22h51m26s	2d45m0s	137 min	0%
A8CRIT	2009-07-13T23:46:15	1003	1	76	22h11m26s	2d45m0s	137 min	0%
A5CRIT	2009-07-13T22:09:07	1001	25	76	21h11m26s	2d45m0s	94 min	0%
B3GALPOL	2009-07-13T19:44:31	999	1	76	12h51m25s	22d7m40s	137 min	100%
B1GALPOL	2009-07-13T18:20:17	997	33	76	12h8m34s	22d7m40s	79 min	98.7%
B1GALPOL	2009-07-13T17:30:30	995	17	33	12h8m34s	22d7m40s	31 min	7.8%
B1GALPOL	2009-07-13T16:43:18	993	1	15	12h8m34s	22d7m40s	27 min	0%
S7	2009-07-13T05:43:36	984	1	24	8h48m0s	-1d0m0s	29 min	10.4%
A11CRIT	2009-07-13T03:35:32	982	1	66	23h11m26s	2d45m0s	119 min	0%
A7CRIT	2009-07-13T01:03:29	980	1	76	21h51m26s	2d45m0s	137 min	0%
A6CRIT	2009-07-12T22:42:21	978	1	76	21h31m26s	2d45m0s	137 min	0%
S7	2009-07-12T22:01:22	976	1	24	8h48m0s	-1d0m0s	29 min	0%
D4GALPOL	2009-07-12T19:15:33	973	1	76	13h14m52s	32d7m40s	137 min	100%
D3GALPOL	2009-07-12T16:14:38	971	1	76	12h51m25s	32d7m40s	137 min	24.1%
D2GALPOL	2009-07-12T13:35:29	969	1	76	12h27m59s	32d7m40s	137 min	0%
D1GALPOL	2009-07-12T11:03:45	967	1	76	12h4m33s	32d7m40s	137 min	0%
C2CIRC	2009-07-12T07:59:32	963	1	76	20h26m55s	72d7m40s	137 min	89.5%
C1CIRC	2009-07-12T05:08:23	961	1	76	19h21m51s	72d7m40s	137 min	100%
A5CRIT	2009-07-12T04:08:53	958	1	25	21h11m26s	2d45m0s	45 min	87.6%
A3CRIT	2009-07-12T01:48:15	956	1	76	20h31m26s	2d45m0s	135 min	29.5%
S7	2009-07-12T01:09:16	954	1	24	8h48m0s	-1d0m0s	29 min	0%
D5GALPOL	2009-07-11T22:38:53	951	1	76	13h38m18s	32d7m40s	137 min	100%
E5GALPOL	2009-07-11T22:17:09	949	67	76	13h41m13s	37d7m40s	18 min	100%
E3GALPOL	2009-07-11T19:55:35	947	1	76	12h51m25s	37d7m40s	137 min	100%
E2GALPOL	2009-07-11T18:14:20	945	27	76	12h26m32s	37d7m40s	90 min	100%
E2GALPOL	2009-07-11T17:04:51	943	1	28	12h26m32s	37d7m40s	50 min	19.9%
S7	2009-07-11T16:19:15	940	1	24	8h48m0s	-1d0m0s	29 min	100%
F1CIRC	2009-07-11T07:50:54	920	1	69	12h51m25s	87d7m40s	124 min	0%
A13CRIT	2009-07-11T05:23:07	917	1	76	23h51m26s	2d45m0s	137 min	36.3%
A9CRIT	2009-07-11T03:00:54	915	1	76	22h31m26s	2d45m0s	137 min	0.4%
A1CRIT	2009-07-11T01:41:32	913	36	76	19h51m26s	2d45m0s	73 min	11.7%
S7	2009-07-11T01:03:53	911	1	24	8h48m0s	-1d0m0s	29 min	0%
E5GALPOL	2009-07-10T22:58:43	909	1	67	13h41m13s	37d7m40s	121 min	100%
A4GALPOL	2009-07-10T20:39:58	907	1	76	13h12m11s	17d7m40s	137 min	100%
A3GALPOL	2009-07-10T18:59:51	905	24	76	12h51m25s	17d7m40s	95 min	78.4%
S7	2009-07-10T18:24:07	903	1	24	8h48m0s	-1d0m0s	29 min	0%
S7	2009-07-10T17:53:16	901	1	24	8h48m0s	-1d0m0s	29 min	0%
S7	2009-07-06T06:14:25	817	1	5	8h48m0s	-1d0m0s	6 min	0%
S7	2009-07-06T05:31:18	814	1	18	8h48m0s	-1d0m0s	22 min	0%
A4CRIT	2009-07-06T02:58:14	812	1	76	20h51m26s	2d45m0s	136 min	46%
A2CRIT	2009-07-06T00:36:01	810	1	76	20h11m26s	2d45m0s	137 min	0%
A2CIRC	2009-07-06T00:15:37	808	74	74	20h57m47s	61d7m40s	5 min	0%
A2CIRC	2009-07-05T22:57:29	807	41	41	20h57m47s	61d7m40s	59 min	0%
A1CRIT	2009-07-05T01:12:59	595	1	35	19h51m26s	2d45m0s	63 min	0%
S7	2009-07-05T00:34:27	593	1	24	8h48m0s	-1d0m0s	29 min	0%
A2CIRC	2009-07-04T06:24:47	457	1	41	20h57m47s	61d7m40s	74 min	100%
A1CIRC	2009-07-04T03:37:44	455	7	7	19h58m50s	61d7m40s	126 min	100%
A1CIRC	2009-07-04T03:18:23	454	1	7	19h58m50s	61d7m40s	13 min	100%
MGALFA1	2009-07-04T00:48:16	452	1	1	23h53m59s	20d10m0s	137 min	0%
ELAISN2	2009-07-03T23:50:37	450	1	24	16h36m58s	41d15m42s	52 min	100%
S7	2009-07-03T23:14:21	448	1	24	8h48m0s	-1d0m0s	29 min	0%
A3GALPOL	2009-07-03T22:24:17	446	1	24	12h51m25s	17d7m40s	43 min	100%
A2GALPOL	2009-07-03T20:04:30	444	1	76	12h30m39s	17d7m40s	137 min	100%
A1GALPOL	2009-07-03T18:45:50	442	36	36	12h9m53s	17d7m40s	74 min	74.5%
A1GALPOL	2009-07-03T16:47:21	438	19	19	12h9m53s	17d7m40s	36 min	0%
A1GALPOL	2009-07-03T16:00:16	435	1	19	12h9m53s	17d7m40s	34 min	0%
S7	2009-07-03T15:20:43	433	1	24	8h48m0s	-1d0m0s	29 min	100%
MGALFA1	2009-06-30T01:59:36	9934	1	1	23h53m59s	20d10m0s	384 min	11.2%

M81BGROUP	2009-06-29T20:53:31	9932	1	46	9h55m32s	69d3m55s	340 min	89.5%
ELAISN3	2009-06-29T19:49:46	9929	1	24	14h29m6s	33d6m0s	53 min	0%
N4490	2009-06-29T18:26:46	9922	1	24	12h30m36s	41d38m22s	29 min	95.1%
S7	2009-06-29T15:47:49	9896	1	24	8h48m0s	-1d0m0s	29 min	100%